THE ASTROPHYSICAL JOURNAL, 495:435–439, 1998 March 1

DISCOVERY OF THE FAINT X-RAY PULSAR AX J1820.5−1434 WITH *ASCA*

K. KINUGASA,[1] K. TORII,[1] Y. HASHIMOTO,[1] H. TSUNEMI,[1,2] K. HAYASHIDA,[1,2] S. KITAMOTO,[1,2] Y. KAMATA,[3] T. DOTANI,[4] F. NAGASE,[4] M. SUGIZAKI,[4] Y. UEDA,[4] N. KAWAI,[5] K. MAKISHIMA,[6] AND S. YAMAUCHI[7]

Received 1997 August 8; accepted 1997 October 10

ABSTRACT

A new X-ray pulsar, AX J1820.5−1434, has been discovered during the *ASCA* Galactic plane survey project on April 9, at R.A. = $18^h20^m29^s.5$, decl. = $-14°34'24''$ (equinox 2000.0; error radius $0'.5$). A coherent pulsation was detected from the source with an apparent barycentric pulse period of 152.26 ± 0.04 s. The mean flux, not corrected for the interstellar absorption, was 2.3×10^{-11} ergs s^{-1} cm^{-2} in the 2–10 keV energy band. The energy spectra obtained by the GIS and SIS can be fitted by a power-law model (photon index = 0.9 ± 0.2) with a large column density of $9.8 \pm 1.7 \times 10^{22}$ H atoms cm^{-2}. These parameters indicate that the new pulsar is a highly obscured accretion-driven binary X-ray pulsar. This discovery of a faint pulsar suggests existence of many hidden pulsars in our Galaxy.

Subject headings: binaries: general — pulsars: general — pulsars: individual (AX J1820.5−1434) — X-rays: stars

1. INTRODUCTION

A coherent pulsation is a strong signature of neutron stars. Accretion-driven X-ray pulsars give us information about various interactions between a neutron star and its environment. So far, 45 X-ray binary pulsars have been discovered (Bildsten et al. 1997) since the first discovery of Cen X-3 with *Uhuru* in 1971 (Giacconi et al. 1971). Among these, more than half (29 sources) are considered to be transients (Bildsten et al. 1997). Therefore, the estimation of the real number of accretion-driven X-ray pulsars is difficult.

The distribution of the accretion-driven bright X-ray pulsars is not concentrated toward the Galactic center region, unlike that of bright low-mass binaries. Also, the distances to the known X-ray pulsars in the Galaxy are distributed within about a few kpc. Therefore, many pulsars lying far from us have not yet been discovered.

A substantially large fraction of the pulsars, especially of the transient pulsars, have a Be companion. Generally, Be stars are active, and large mass transfer is expected. This means that there might be many faint pulsars, undiscovered because their companions are not Be stars and have small activity.

Koyama et al. (1990) pointed out a "colony" of X-ray pulsars in the 5 kpc Galactic arm (Scutum arm), especially in the Scutum region, based on their discovery of four pulsars and three hard transient sources (Koyama et al. 1989, 1991). Yamauchi et al. (1995) further discovered a new transient X-ray source in the Scutum region with *ASCA*. Most of these sources are relatively faint, with a flux of few mcrab and with a large absorption column density of roughly 10^{23} H atoms cm^{-2}. In other Galactic plane regions, a transient pulsar, X1722-36 (Tawara et al. 1989) has been reported. It is also highly obscured, with a column density of about 10^{24} H atoms cm^{-2}.

One of the main scientific objectives of the now ongoing *ASCA* Galactic plane survey project (e.g., Koyama et al. 1997; Sugizaki et al. 1997a, 1997b; Kinugasa et al. 1997; Kaneda 1997) is to search for faint pulsars. The wide and high-energy band (up to 10 keV) X-ray imaging capability and the high spectral resolving power of *ASCA* will make it possible to detect faint and obscured pulsars in the Galactic inner disk. In this paper we report the discovery of an X-ray pulsar, AX J1820.5−1434 (Torii, Kinugasa, & Kitamoto 1997) near the Scutum region.

2. OBSERVATIONS

The *ASCA* Galactic plane survey project started from the AO-4 period and will be continued during the full *ASCA* mission life of several yr. This project plans to cover the entire Galactic inner disk ($|l| < 45°$ and $|b| < 0°.8$), with successive pointing observations of regions 50′ in diameter, with about 10 ks exposure for each.

The first AO-5 survey, made in 1997 April 8–12, covered the regions of $l = 16°.0$–$20°.5$ along $b = 0°$. The new X-ray pulsar was discovered when the field of view (FOV) was centered at $l = 16°.5$, $b = 0°$ on 1997 April 9.

The new pulsar was observed with the two CCD cameras (designated as SIS0 and SIS1; Burke et al. 1994) and two imaging gas scintillation proportional counters (designated as GIS2 and GIS3; Ohashi et al. 1996; Makishima et al. 1996), placed at the focal plane of four thin-foil X-ray mirrors (XRT; Serlemitsos et al. 1995) on board *ASCA* (Tanaka et al. 1994).

The SIS data were obtained with the 4-CCD Faint/Bright mode covering a FOV of $\sim 22' \times 22'$ with a level discrimination of 1.1 keV, while the GIS data were taken in the normal PH mode with a circular FOV of 25′ radius and a time resolution of 62.5 ms (high bit rate) or 0.5 s (medium bit rate). We excluded the GIS data obtained in the South Atlantic Anomaly (SAA), the Earth occultation, high-background regions at low geomagnetic cutoff rigidities of less than 6 GeV c^{-1}, and the elevation angle from the Earth rim of less than 10°. We applied a rise-time discrimination

[1] Department of Earth and Space Science, Graduate School of Science, Osaka University, 1-1 Machikaneyama-cho, Toyonaka, Osaka 560, Japan.
[2] CREST, Japan Science and Technology Corp. (JST).
[3] Department of Astrophysics, Nagoya University, Furo-cho, Chikusa-ku, Nagoya 464-01, Japan.
[4] Institute of Space and Astronautical Science, 3-1-1 Yoshinodai, Sagamihara Kanagawa 229, Japan.
[5] Institute of Physical and Chemical Research (RIKEN), 2-1 Hirosawa, Wako, Saitama 351-01, Japan.
[6] Department of Physics, University of Tokyo, Bunkyo-ku, Tokyo 113, Japan.
[7] Faculty of Humanities and Social Sciences, Iwate University, 3-18-34 Ueda, Morioka, Iwate 020, Japan.

technique to reject particle events in the GIS data. For the SIS data we excluded those during the SAA, the Earth occultation, regions of low cutoff rigidities (less than 6 GeV c^{-1}), and the elevation angle from the night and day Earth rim of less than 10° and 25° for SIS0, and less than 10° and 20° for SIS1, respectively. Only the faint-mode data were analyzed, because the Residual Dark Distribution (RDD) correction (Yamashita 1997; Dotani et al. 1997) is available for the faint-mode data. After the RDD correction, the nominal PH corrections (echo, Dark Frame Error [DFE], and Charge Transfer Inefficiency [CTI] corrections; see Otani & Dotani 1994) were made. The events with grades of 0, 2, 3, and 4 were used for this analysis. The net exposure time is 10.5 ks for GIS and 4.8 ks for SIS, spanning about 27 ks (MJD = 50547.27–50547.58).

3. ANALYSIS AND RESULTS

3.1. *Source Identification and Background Estimation*

In the GIS X-ray image shown in Figure 1 we clearly found a point source at the sky position

$$\text{R.A.(J2000)} = 18^{\mathrm{h}}20^{\mathrm{m}}29\overset{\mathrm{s}}{.}5;\ \text{decl.(J2000)} = -14°34'24'' ;$$

$$(l, b) = (16\overset{\circ}{.}472,\ 0\overset{\circ}{.}070) .$$

The above position is accurately determined with the SIS image by the results of the recent *ASCA* alignment calibration and has an error radius of 0'.5 (Y. Ueda 1997, private communication). Therefore, we designated this source as AX J1820.5−1434. Since no cataloged X-ray source has been found within the error region of this source (e.g., Voges et al. 1996; *ROSAT* All Sky Survey), we conclude that AX J1820.5−1434 is a new X-ray source.

Since the obtained data were contaminated by the heavy stray light from GX 17+2, we carefully estimated the background of the GIS data for further analysis. The stray light profile is roughly a circular shape centered at the bright source GX 17+2. The smoothed stray light has a gradual intensity variation along the azimuthal direction. Two spectra for the GIS background were made from two regions on the stray light circle shown in Figure 1: GIS-BGD1, a circular region with a radius of 6' centered at (R.A., decl.) (J2000) = ($18^{\mathrm{h}}20^{\mathrm{m}}33\overset{\mathrm{s}}{.}7$, −14°24'00'') and GIS-BGD2, circular region with a radius of 6' centered at (R.A., decl.) (J2000) = ($18^{\mathrm{h}}20^{\mathrm{m}}06\overset{\mathrm{s}}{.}2$, −14°42'39''). GIS-BGD1 is at a relatively bright region, and GIS-BGD2 is at a faint region. The flux of GIS-BGD2 is ∼75% of that of GIS-BGD1 in both the 2–5 and 5–10 keV bands. Since the intensity of the stray light gradually decreases along the azimuthal direction, the background level of the source region is ∼10%–15% lower than GIS-BGD1, while because of the vignetting effect, the background level around the source should be about 15% brighter than GIS-BGD1. We will use GIS-BGD1 as the background in further analysis. The ambiguity of the background level is thus less than 15%.

The source data both for the GIS and SIS were extracted from the circular regions with a radius of 4' centered at the source position. Background data for the SIS were made from the annulus region with a radius of 4'–7' around the source (Fig. 1), because we could not extract the background from GIS-BGD1, owing to the limited FOV of SIS. Although the background region for the SIS analysis is different from that of the GIS, the amount of the background uncertainty is roughly the same as that of the GIS, since it is determined by the stray light structure.

Most of the X-ray photons from AX J1820.5−1434 are in the energy range of 3–10 keV. The raw counts (including the background) of the source region within the energy band are 3567 and 1362 for GIS2 + 3 and SIS0 + 1, respectively. The background counts in the same region and the same energy band are estimated to be about 900 and 370 for GIS2 + 3 and SIS0 + 1. These are about 25%–27% of the total counts of the source region. The uncertainty of the background of about 15% corresponds to 4% of the total flux of the source region.

3.2. *Timing Analysis*

To search for the coherent pulsation, we calculated a power spectral density (PSD) by using the GIS data, after barycentric corrections for the photon arrival times. A fast Fourier analysis to obtain the PSD was performed up to the Nyquist cutoff frequency of 8 Hz for high–bit-rate data and of 1 Hz for high– and medium–bit-rate data. The resultant PSD is shown in Figure 2. In the PSD a coherent oscillation with a fundamental frequency of about 0.00657 Hz was found. We also calculated the PSD of the data from the GIS-BGD1 and found no significant peak. Therefore, we conclude that the coherent pulsation originates from the source. In order to determine the pulse period accurately, we used a folding technique with the assumption of a constant period, and we found a pulse period of 152.26 ± 0.04 s. The error of the period is limited by the relatively short exposure (∼10 ks) and span (∼27 ks). The folded pulse profiles are shown in Figure 3 in the 2–5 and 5–10 keV bands, where the background was subtracted, assumed to be constant, and phase 0 was defined to be MJD 50547.00 after barycentric corrections. The hardness ratio of the two energy bands is also plotted in Figure 3. The pulse shape has one broad peak with a phase width of 0.3. At the peak the pulsed flux is roughly twice the flux of the constant component. No significant change of the hardness ratio was found at the 90% confidence level.

We divided the data into two sets, the first half (MJD = 50547.27–50547.43) and the second half (MJD = 50547.44–50547.58), and determined the pulse period separately using the folding technique. The resultant periods are 152.26 ± 0.11 and 152.31 ± 0.10 s, respectively. Therefore, the apparent period derivative is less than 2.5×10^{-5} s s^{-1}.

3.3. *Spectrum Analysis*

Using both the GIS and the SIS data, we extracted the X-ray spectra from the same region as the above timing analysis data. The background-subtracted phase-averaged spectra are shown in Figure 4. We simultaneously fitted the spectra obtained by each sensor with the two conventional models: a power law and a blackbody taking into account the interstellar absorption (Morrison & McCammon 1983). The best-fit spectral parameters are summarized in Table 1. Both models gave acceptable fits. A notable result is the heavy absorption of about 0.5–1 × 10^{23} H atoms cm^{-2} for two models. Since the spectra of X-ray pulsars were conventionally fitted with the power-law model (e.g., Nagase 1989; Koyama et al. 1990), we used the power-law model for the further spectral analysis.

To search for the iron line structures, we try to fit the spectra with a power law plus narrow emission lines at 6.4,

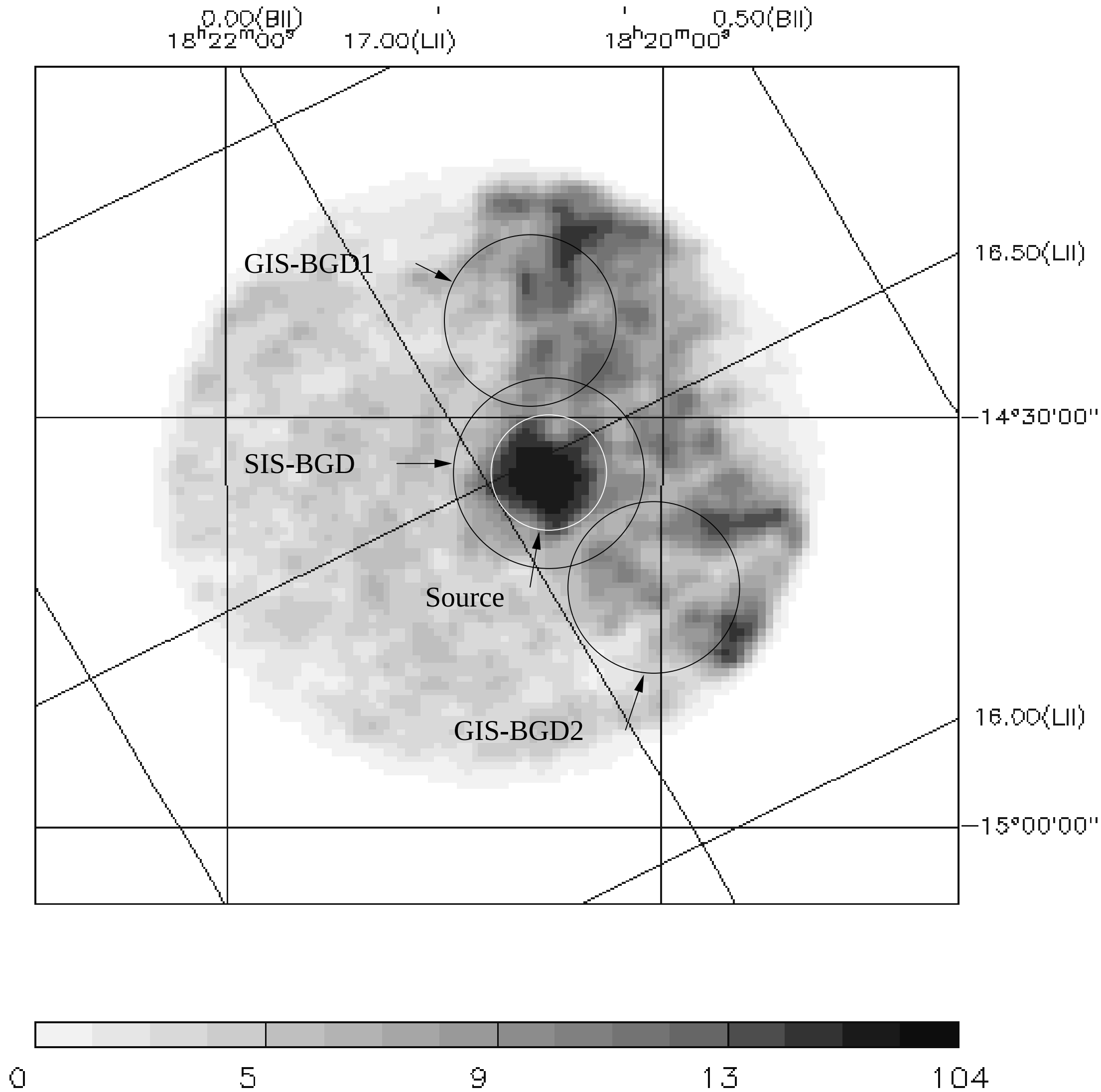

FIG. 1.—GIS image of the field of view, including AX J1820.5−1434, with an energy range of 0.7–10 keV. The sky coordinate is in J2000. A stray light from a bright binary X-ray source contaminates the field of view. The background regions and the source region for the analysis were also plotted. The background is not subtracted and the vignetting is not corrected for.

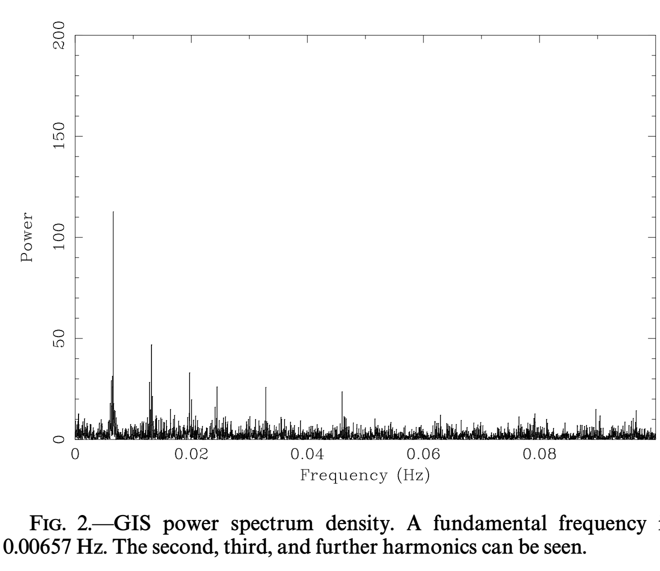

FIG. 2.—GIS power spectrum density. A fundamental frequency is 0.00657 Hz. The second, third, and further harmonics can be seen.

6.7, and 6.9 keV, which respectively correspond to Kα lines of neutral, He-like, and H-like iron ions. Though we did not find the latter two, we found a significant neutral iron line with 95% confidence. The equivalent widths of the neutral, He-like, and H-like lines are 90 (15–170) eV, less than 70 eV, and less than 50 eV, respectively, where errors and upper limits are at 90% confidence levels.

The observed and absorption-corrected fluxes in the 2–10 keV band are estimated to be $\sim 2.3 \times 10^{-11}$ ergs cm^{-2} s^{-1} and $\sim 3.3 \times 10^{-11}$ ergs cm^{-2} s^{-1}; the latter corresponds to the luminosity of $\sim 4 \times 10^{35}(D/10\ \mathrm{kpc})^2$ ergs s^{-1}, where D is the distance to the source.

The light curve of the source was derived from the spectral fitting analysis. We divided the GIS data into 10 subsets and extracted the spectra of each subset. In Figure 5 we plotted the fluxes derived from the best-fit power-law model of the 10 phase-averaged spectra. The hypothesis that the flux is constant is acceptable for the 95% confidence level,

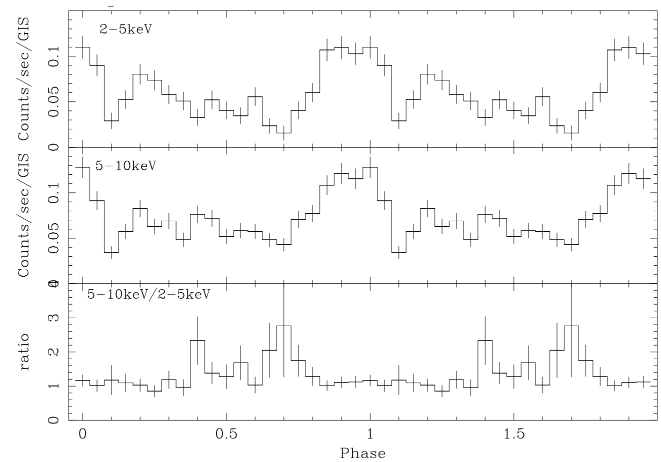

FIG. 3.—Folded light curves in the energy range of 2–5 keV and 5–10 keV and their hardness ratio. The background GIS-BGD1 is subtracted. Phase 0 is defined to be MJD 50547.00.

but not acceptable for the 90% level, marginally suggesting a trend of gradual increase of the flux during the observation.

In order to study the spectral variation in the spin phase,

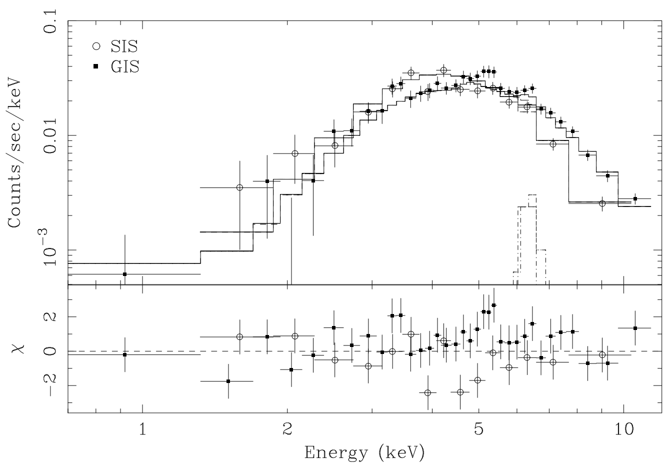

FIG. 4.—Phase-averaged spectra (*crosses*) and best-fit power law plus Gaussian model curves (*histograms*). Each data point is an averaged datum of two SIS and of two GIS sensors.

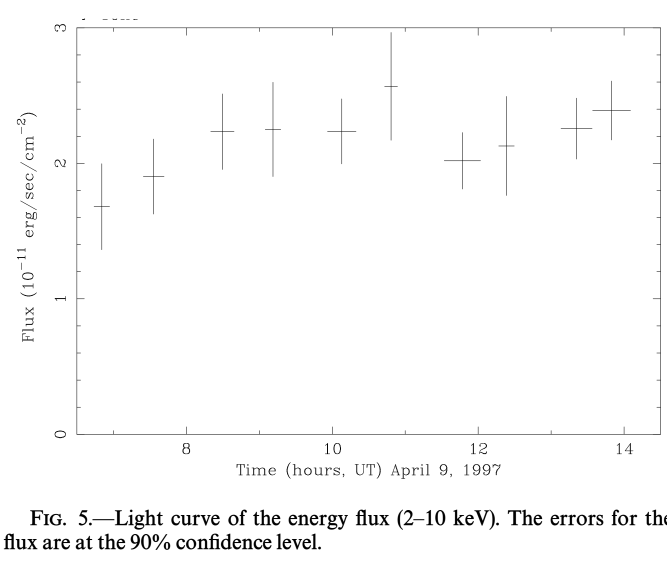

FIG. 5.—Light curve of the energy flux (2–10 keV). The errors for the flux are at the 90% confidence level.

TABLE 1

THE BEST-FIT PARAMETERS OF THE PHASE-AVERAGED SPECTRA

Parameter	Best-Fit Value
Blackbody	
kT (keV)	2.6 (2.4–2.9)
R^2/D_{10}^2 (km^2)[a]	0.10 (0.07–0.13)
N_H (10^{22} cm^{-2})	5.6 (4.6–6.8)
Reduced χ^2 (dof)...........	1.054 (274)
Power Law	
Γ_{ph}[b]	0.9 (0.7–1.1)
Norm[c]	2.2 (1.5–3.3)
N_H (10^{22} cm^{-2})	9.8 (8.2–11.5)
Reduced χ^2 (dof)...........	1.035 (274)
Power Law + Gaussian[d]	
Γ_{ph}[b]	0.9 (0.7–1.1)
Norm[c]	2.1 (1.4–3.3)
N_H (10^{22} cm^{-2})	9.5 (8.0–11.2)
E_{line} (keV)	6.4 (fixed)
EW (eV)	90 (15–170)
Reduced χ^2 (dof)...........	1.025 (273)

NOTE.—The errors are at the 90% confidence level ($\Delta\chi^2 < 2.7$ for one parameter), which does not include the systematic error resulting from subtracting the background.

[a] R is the radius, and D_{10} is $D/10$ kpc, where D is the distance to the source.

[b] Photon index.

[c] In units of 10^{-3} photons keV^{-1} cm^{-2} s^{-1} at 1 keV.

[d] Since we assumed narrow line, the intrinsic line width is fixed at 0.

we extracted two pulse-phase–sliced spectra: 0.2–0.7 (a low-intensity phase) and 0.7–0.2 (a high-intensity phase). We fitted a power law and a power law plus Gaussian model. No significant differences in the power indexes and in N_H value were found, consistent with the lack of significant change of the hardness ratio shown in Figure 3.

4. DISCUSSION

AX J1820.5−1434 is the second newly discovered pulsar in the *ASCA* Galactic plane survey project, the first being 1RXS J170849.0−400910 (Sugizaki et al. 1997a, 1997b). AX J1820.5−1434 is between the Galactic center and the Scutum region, which was pointed out as a "colony" of X-ray pulsars. The obtained absorption column density was $\sim 10^{23}$ H atoms cm^{-2}, which is roughly the same value as that of the other Scutum region sources (Koyama et al. 1990; Yamauchi et al. 1995). This implies that the newly discovered pulsar is also at a similar distance. If the source is on the Scutum arm, then the distance to the source is $\sim$4.7 or $\sim$11.7 kpc, which are the distances of the two cross points of the Scutum arm and our line of sight, assuming an 8.5 kpc distance to the Galactic center. Then the luminosity after correction for the interstellar absorption is about 9×10^{34} ergs s^{-1} or 5×10^{35} ergs s^{-1}. The spectral properties of the source, a power law with a photon index of 0.9 ± 0.2 and a 6.4 keV iron line with the equivalent width of $\sim$100 eV, in the energy range of 1–10 keV, are typical features of an accretion-driven X-ray pulsar (e.g., Nagase 1989). The X-ray luminosity of the source is similar to that of other Scutum region sources (Koyama et al. 1990), but it is a rather faint value, compared to the typical luminosities ($\sim 10^{36}$–10^{37} ergs s^{-1}) of known X-ray pulsars (Nagase 1989).

Although this source region was observed in the *ROSAT* All Sky Survey in 1990–1991, the source was not detected at the time. If the source had similar flux during the *ROSAT* survey, it might not be detected because of the large absorption. The estimated count rate of the PSPC on board *ROSAT*, from the best-fit spectra of this observation, is below 0.001 counts s^{-1}, which is below the detection limit (0.05 counts s^{-1}) of the *ROSAT* All Sky Survey (Voges et al. 1996). The region has been observed in the *Ginga* survey project (e.g., Koyama et al. 1989). The estimated count rate of the LAC on board *Ginga* is about 10 counts s^{-1}, and this is above the detection limit (2 counts s^{-1}) of the *Ginga* survey. However, since LAC is a nonimaging detector, and the scan paths are parallel to the Galactic plane, the *Ginga* survey was unable to distinguish this source from GX 17+2, $(l, b) = (16\overset{\circ}{.}4, 1\overset{\circ}{.}3)$ (S. Yamauchi 1997, private communication). During this observation span, the long term flux variation was not clearly found. Therefore, it is not clear whether this new pulsar is a transient source or a faint persistent source.

Thirteen of the 29 transient pulsars have been established as having a Be star companion. This large fraction might result from an activity of the Be star companion. If so, there may be many pulsars that are not associated with a Be star and have not yet been observed because of their low luminosity. This newly discovered faint pulsar may be a member of this new class of binary pulsars. Therefore, it is important to determine the spectral type of the companion star of this pulsar by optical observations.

The discovery of this pulsar encourages the search for other low-luminosity and heavily obscured X-ray pulsars on the Galactic plane. The wide and hard X-ray imaging capability of *ASCA* makes possible the discovery of these new faint pulsars. The characteristics of this faint pulsar are not yet clear; further deep and long-term observation and the determination of the spectral type of the companion star are required.

The authors are grateful to all the members of the *ASCA* team. In particular, we thank the *ASCA* Galactic plane survey project team for their support and discussions of this work.

REFERENCES

Bildsten, L., et al. 1997, ApJS, 113, 367
Burke, B. E., Mountain, R. W., Daniels, P. J., Cooper, M. J., & Dolat, V. S. 1994, IEEE Trans. Nucl. Sci., 41, 375
Dotani, T., Yamashita, A., Ezuka, E., Takahashi, K., Crew, G., Mukai, K., & the SIS team 1997, *ASCA* News, 5, 14
Giacconi, R., Gursky, H., Kellogg, E., Schreier, E., & Tananbaum, H. 1971, ApJ, 167, L67
Kaneda, H. 1997, Ph.D. thesis, The University of Tokyo
Kinugasa, K., Torii, K., Tsunemi, H., Yamauchi, S., Koyama, K., & Dotani, T. 1997, PASJ submitted.
Koyama, K., et al. 1989, PASJ, 41, 483
Koyama, K., Kawada, M., Kunieda, H., Tawara, Y., Takeuchi, Y., & Yamauchi, S. 1990, Nature, 343, 148
Koyama, K., Kunieda, H., Takeuchi, Y., & Tawara, Y. 1991, ApJ, 370, L77
Koyama, K., et al. 1997, PASJ, 49, L7
Makishima, K., et al. 1996, PASJ, 48, 171
Morrison, R., & McCammon, D. 1983, ApJ, 270, 119
Nagase, F. 1989, PASJ, 41, 1
Ohashi, T., et al. 1996, PASJ, 48, 157
Otani, C., & Dotani, T. 1994, *ASCA* News, 2, 25
Serlemitsos, P. J., et al. 1995, PASJ, 47, 105
Sugizaki, M., et al. 1997a, IAU Circ. 6585
Sugizaki, M., et al. 1997b, PASJ, 49, L25
Tanaka, Y., Inoue, H., & Holt, S. S. 1994, PASJ, 46, L37
Tawara, Y., Yamauchi, S., Awaki, H., Kii, T., Koyama, K., & Nagase, F. 1989, PASJ, 41, 473
Torii, K., Kinugasa, K., & Kitamoto, S. 1997, IAU Circ. 6678
Voges, W., et al. 1996, IAU Circ. 6420
Yamashita, A., et al. 1997, IEEE Trans. Nucl. Sci., 44, 847
Yamauchi, S., et al. 1995, PASJ, 47, 189